JOURNAL OF MATERIALS SCIENCE 16 (1981) 313–330

Molecular dynamics simulation of mechanical behaviour

E. D. SHCHUKIN, V. S. YUSHCHENKO
The Institute of Physical Chemistry, Academy of Sciences of the USSR, Moscow, Leninski Prospekt 31, USSR

A molecular dynamics (MD) simulation of strain and failure of a crystal, the effect of environment on these processes, the interaction between the adsorption-active atoms and the environment walls, the effect of stress on mobility of interstitial admixtures, the formation and the failure of a contact between two crystals has been performed using a two-dimensional system consisting of Lennard–Jones atoms. The basic features of strain observed by means of MD included generation and motion of dislocations, various mechanisms of shear and brittle-to-ductile transition at low temperature. Environment-sensitive mechanical behaviour has been studied for the first time on an atomic scale. It is shown that rapid local processes whose unit act takes about 10^{-10} sec and involves several tens or a few hundred atoms may provide for environment-induced embrittlement. The features common to these microscopic processes are (1) pronounced interaction between the foreign atoms and the atoms of the solid, i.e. a sharp decrease in the surface energy of the solid in contact with the environment, and (2) direct participation of thermal fluctuations in the failure and rearrangement of interatomic bonds. By interacting with the crack walls, the environment atoms create a force compatible with the interatomic bond strength, which promotes crack propagation. Tensile stress causes appreciable acceleration of diffusion of interstitial admixtures in the direction normal to the strain axis and hinders diffusion along the axis. Under constant load the failure of interatomic bonds and sintering involve a thermal fluctuation mechanism.

1. Introduction

The understanding of the Rehbinder effect requires information on the atomic-scale mechanisms of adsorption-sensitive mechanical behaviour. In solving this problem one faces both experimental and theoretical limitations. No experimental technique can provide for the direct observation of the gradual stepped movement of individual atoms (molecules) taking part in the thermal motion. Theoretical methods including computer calculations, on the other hand, routinely involve certain *a priori* models which essentially simplify the actuall processes.

These limitations may be to a certain extent overcome with the help of the molecular dynamics (MD) approach, which deals with an ensemble of several tens or hundred of atoms (molecules) possessing a certain mass and size and arranged in a preset initial order. Other parameters of such a system include the interaction potential between the particles, the kinetic energy (temperature) of the system expressed in terms of the initial random distribution of their pulses and the potential of interaction between the particles and the environment, such as the walls of the "box" containing the ensemble. By integrating the Newtonian equations of motion of all the particles according to a preset program a computer can calculate their co-ordinates, pulses and interactions, as well as such overall characteristics as the potential and the kinetic energies of the system, the work of the applied force, etc. These stepped calculations make it possible to obtain a unique dynamic picture of the process and to observe the behaviour

0022–2461/81/020313–18$03.80/0

of all the atoms involved, which is the main advantage of MD over other combinations of experimental and theoretical techniques.

The technique of molecular dynamics was suggested more than two decades ago by Alder and Weinwrite [1] and Rahman [2]. Its general features, as well as the numerous applications for the analysis of many physico-chemical phenomena were recently reviewed by Wood and Erpenbeck [3] whose otherwise comprehensive paper, unfortunately, fails to mention a number of Soviet works in the field (Yevseev *et al.* [4–6], Lagar'kov and Sergeev [7–9], Grivtsov Shnol' *et al.* [10–13] etc). The last-named group of workers was the first to undertake a MD study of surface phenomena and adsorption. In co-operation with Grivtsov, the authors of the present paper used the MD approach to investigate the molecular mechanisms of some physico-chemical processes on solid surfaces, namely wetting and spreading [14, 15], deformation and failure of crystals [16, 17] and the effect of foreign atoms (environment) on these processes [18].

The present paper is only concerned with the mechanical behaviour of materials. The technique of computer experiments with two-dimensional crystals is described briefly in Section 2. Section 3 deals with such problems as the molecular-scale picture of elastic deformation and plastic flow of these crystals, the emergence of defects and crack propagation at various temperatures and under different conditions of strain. The unit processes of environment-assisted failure, i.e. the mechanism of adsorption-induced strength reduction (the Rehbinder effect) will be discussed in Section 4. Interaction of the environment atoms with the crack walls will be discussed in Section 5. The effect of stress on the diffusion rate and on the solubility of interstitial admixtures is considered in Section 6 and the long-term strength of an individual atomic bond (static fatigue measurements) is considered in Section 7. Finally, Section 8 concerns the early stages of crystal sintering, which involves the emergence and failure of unit phase contacts.

Within the limits of this brief review the authors confined themselves to the description of the most important results, particularly the observed atomic-scale pictures of the processes. Quantitative estimations, though quite possible using the MD approach, prove fairly time-consuming in the case of non-stationary behaviour. Thus our description is primarily qualitative. However, a certain body of quantitative information such as the strength of a two-dimensional crystal, changes in temperature during deformation, the dislocation velocity and some other evaluations will be reported below; the details may be found in our earlier papers [16–22].

2. Experimental procedure

The investigation involved two-dimensional systems, so that the number of particles was limited (~ 200) and the count time reasonable. The results could be easily visualized since the computer gave the co-ordinates of every atom at regular intervals, which was especially valuable in the case of the processes involving mutual displacement of atoms. Two-dimensional systems, of course, differ from three-dimensional ones in several ways (for example, consider the instability of infinite [23] or even very large [24] two-dimensional crystals). Nevertheless, there is considerable evidence obtained from computer experiments that two-dimensional systems display many basic features of their three-dimensional counterparts.

The atoms were assumed to interact via the Lennard–Jones potential $\varphi(r) = \epsilon[(r_0/r)^{12} - 2(r_0/r)^6]$*. This potential is widely used in MD calculations and usually refers to noble gases. It was also shown to be valid for the description of certain properties of Ti, Be, Mg and other hexagonal close-packed metals [25]. Since the Rehbinder effect is now known to be common to virtually all types of solids [26–28] it could be expected that the two-dimensional crystals consisting of Lennard–Jones atoms would also manifest the principal features of adsorption-induced strength reduction.

In their preset initial positions the atoms formed a h c p lattice cell placed in a box (ABCD, Fig. 1) whose walls interacted only with the nearest layer of atoms via the 9–3 potential. The walls parallel to the close-packed atomic layers (AB and CD) were mobile and their interaction with the atoms was strong enough to prevent the separation of the particles from the walls during deformation. The second pair of walls was immo-

*Truncated potentials were used. The truncating radius for atomic interactions was $r_c = 3r_0$, for atom-wall interaction $r_c = 1.3r_0$. To improve the conservation of overall energy the potentials were corrected, i.e. the value $\varphi(r) - \varphi(r_c)$ was used as the potential.

bile and their interaction with atoms was weak. They did not allow the atoms to spread over the AB and CD walls. In the absence of strain such a system is stable and develops spontaneously from, for instance, the state when the close-packed rows are parallel to the weakly interacting walls. Deformation was accomplished by moving the AB and CD walls apart so that the centre of gravity was at rest. During the experiments the main events occurred in the middle of the box and were thus fairly independent of the type and parameters of the atom–wall interaction potentials.

Both the magnitude and the direction of the initial pulses of the atoms were preset at random. The distribution of pulse projections on the axes (uniform or normal) proved insignificant, since the system reached thermal equilibrium rapidly enough. The overall kinetic energy corresponded to a certain preset value, the velocity of the centre of masses was zero.

All the numerical values in this paper are expressed in terms of the interaction potential parameters and the mass of the basic component (B) atoms, i.e. ϵ_{BB}, r_0^{BB} and m_B^*. Thus the energies are measured in ϵ units, the distances in r_0, the times in $r_0(m/\epsilon)^{1/2}$, velocities in $(\epsilon/m)^{1/2}$, forces in ϵ/r_0, or, in a more illustrative manner, in unit interatomic bond strengths $F_m = -(\mathrm{d}p/\mathrm{d}r)_{max} \approx 2.69\,\epsilon/r_0$. For argon, a typical object of MD calculations, $\epsilon = 119.8\,\mathrm{K} = 1.654 \times 10^{-14}\,\mathrm{erg}$, $r_0 = 3.82\,\text{Å}$, $m = 6.64 \times 10^{-23}\,\mathrm{g}$, $r_0(m/\epsilon)^{1/2} = 2.42 \times 10^{-12}\,\mathrm{sec}$, $(\epsilon/m)^{1/2} = 1.58 \times 10^4\,\mathrm{cm\,sec^{-1}}$, $\epsilon/r_0 = 4.33 \times 10^{-7}\,\mathrm{dynes}$ and $F_m = 1.165 \times 10^{-6}$ dynes.

The equations of motion were integrated using the method of central differences with the step $r_0(m/\epsilon)^{1/2}/64$. The total energy of the system minus the work performed by the applied force was constant to within 0.3%. The calculations were carried out using M-222 and BESM-6 computers employing an assembly program.

3. Deformation of a single-component crystal

The system used to study the general picture of strain and failure of a two-dimensional microcrystal is shown in Fig. 1. In this series of experiments the central cavity served as a mere stress concentrator, while otherwise it contained atoms of a foreign component (see Section 4). The system

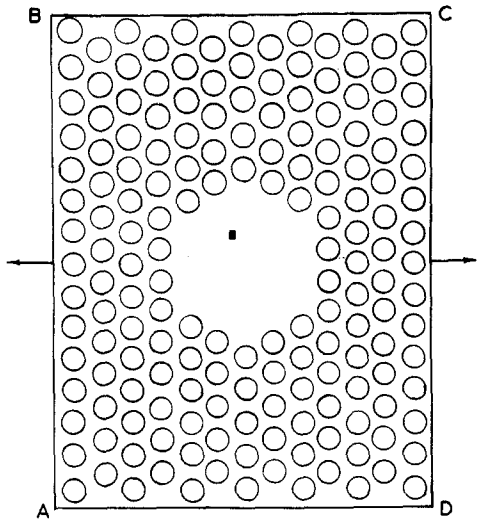

Figure 1 The initial positions of the atoms. The rectangle in the centre corresponds to the accuracy of the atomic co-ordinates.

was deformed by moving the AB and CD walls apart at a constant speed; the changes brought about by strain were observed in the pictures by the positions of the particles. Also measured were the potential energy, the kinetic energy and the forces applied to the box walls. The experiments were characterized by variables such as the strain rate [from 0.03 to $0.3\,(\epsilon/m)^{1/2}$], the initial kinetic energy, the temperature (kT from 0 to $0.2\,\epsilon$) and the distribution of inital atomic velocities. The observation time was long enough for the system to accomplish a unit act of strain and failure (depending on the strain rate, from 10 to $100\,r_0(m/\epsilon)^{1/2}$, which in the case of argon corresponds to 2.4 to 24×10^{-11} sec).

Slow deformation involves regular changes in the force applied to the mobile walls (Fig. 2). The early linear stage refers to elastic deformation (Stage I in Fig. 2). The Young's modulus calculated from these data and from the geometry of the crystal is equal to $\approx 80\,\epsilon r_0^2$, just slightly less than the theoretical prediction [29, 30] (because of the relatively major strain and non-zero temperature) and is in agreement with the experimental results for solid argon [31].

As structural defects appear and accumulate in the lattice, deformation is no longer linear (Stage II in Fig. 2). The initial stage of this process consists of the bending of the atomic rows, parti-

*In the discussions of single-component systems the BB superscripts were omitted for the sake of simplicity. In two-component systems the second component (the adsorption-active environment) is denoted by A.

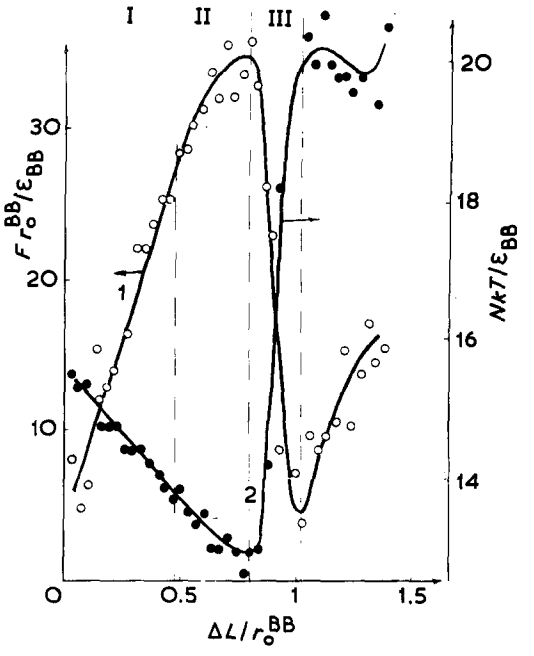

Figure 2 The force applied to the mobile walls (1) and the kinetic energy (temperature) of the system (2) plotted against the deformation. The displacement velocity of the walls is $0.03 \times (\epsilon/m)^{1/2}$.

cularly those tilted at 30° to the strain axis. As the tensile force reaches its maximum, other defects appear, primarily dislocations (e.g. AB line in Fig. 3). For a certain period of time after appearing at the surface of the cavity a dislocation

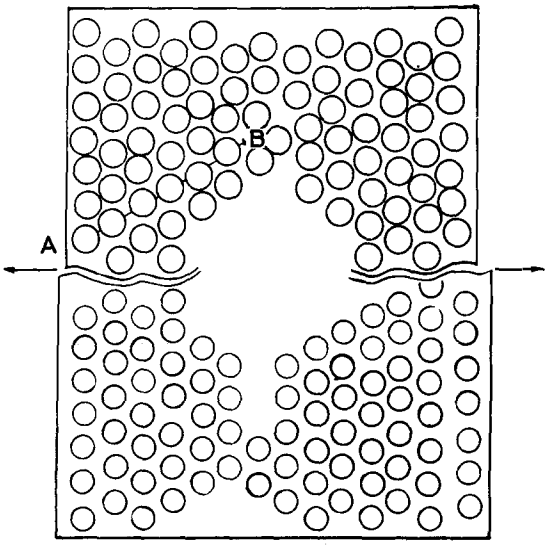

Figure 3 Formation of a dislocation (above) and brittle cracking (below) during deformation. The results of experiments at high and low temperatures respectively.

is moving in the close-packed atomic row ("slip plane"). Since the geometry of the system does not permit the dislocation to emerge on an immobile (weakly interacting) wall, the non-conservative movement and generation of vacancies is observed. The vacancies usually emerge on the immobile wall. The dislocation velocity in the slip plane, as estimated from the pictures of atomic positions, proved equal to about $2r_0(m/\epsilon)^{1/2}$, which is several times lower than the velocity of sound. Changes in temperature did not affect the dislocation velocity. Our estimation of this value is but approximate; in a special study the dislocation velocity at different temperatures and under different stresses may be measured with a fair degree of accuracy.

As the initial system contained no dislocation sources, its strength was almost ideal and deformation did not necessarily involve the dislocation mechanism. The alternative mechanisms observed under identical strain rate and temperature conditions in systems with different sets of random atomic velocities included simultaneous shear along the entire slip plane with subsequent failure near the immobile wall. This agrees with the geometry of the system, lattice decay across the whole neck (local melting), substantial rearrangement of the atoms and a variety of intermediate mechanisms when, for example, a dislocation proved "scattered" over several interatomic distances. Whether a particular strain behaviour would take place is a statistical event, each mechanism having its own probability and the dislocation mechanism being considerably more likely than the others. Thus, sometimes during simultaneous deformation, either neck of the microcrystal studied displayed its own strain mechanism. This microscopic "variability" of the process emphasizes the experimental nature of the MD approach. One cannot therefore impose a particular mechanism on the process if another strain mechanism can operate under the given conditions. On the other hand, this factor suggests that the basic paths of the process may be revealed only in a large series of experiments. Also quantitative estimations by means of the MD method may be difficult to obtain, as they are to be averaged over individual unit acts of the process rather than over time as is usual with stationary systems.

The above-described irreversible strain causes a decrease in the tensile force (stress relaxation, Stage III in Fig. 2). The relaxation time $\approx 4r_0(m/\epsilon)^{1/2}$ takes a few thermal vibration periods of atoms

$[\approx 0.4r_0(m/\epsilon)^{1/2}]$. The stress relaxation results in the almost ideal restored lattice with an additional row of atoms and with thinner necks. During further deformation the picture is reproduced several times, but as the necks between the mobile walls become thinner, the tensile force gradually decreases.

At the hypothetical temperature, 0 K, when the atoms in the initial state are immobile the system displayed a ductile-to-brittle transition. On passing from Stage II to III the bends of atomic rows form a crack (Fig. 3) which crosses almost the whole sample. By the time the crack emerges on an immobile wall the temperature of the system increases appreciably and the weakly-bound surface atoms fill the crack tip. Generally speaking, brittleness is not characteristic of a two-dimensional crystal, and at temperatures as low as $kT = 0.01\,\epsilon$ the deformation was always ductile.

The temperature of the system during deformation is not constant (Fig. 2, Curve 2). The system is adiabatic and the stored elastic energy released during stress relaxation transforms into heat. Of particular interest is the fact that during elastic deformation the crystal cools down, which indicates that elastic energy accumulates on account of the kinetic energy of atoms as well as due to the work of the applied force. However intriguing it may seem, this effect has a simple thermodynamical explanation: the reversible extension of a solid possessing a positive thermal expansion ratio involves heat absorption in isothermal systems and cooling in adiabatic systems. If the Carneau cycle is considered (isothermal expansion, adiabatic extension, isothermal compression, adiabatic compression) and if it is assumed that temperature variations in adiabatic processes are proportional to the changes in stress, a correlation between the heat absorption during isothermal extension (δQ), cooling during adiabatic extension (ΔT) and the variation of stress (Δp) is obtained

$$\delta Q = v\alpha T\Delta p; \quad \Delta T = -\frac{\alpha \bar{T}}{c}\Delta p, \qquad (1)$$

(tensile stress is assumed positive) where v is the volume of the sample, α is the linear expansion ratio, c is the heat capacity per unit volume under constant stress and $\bar{T} = (T_1 + T_2)/2$ is the average temperature of the adiabatic process.

If the strain rate exceeds $0.2\,(\epsilon/m)^{1/2}$, the walls of the box move so far apart during relaxation that the stress again reaches the value of the crystal strength, and Stage III overlaps with Stage I of the next act of deformation. The behaviour becomes more complex: while some defects heal, other ones appear, the cleavage along close-packed atomic rows and the local decay of the lattice become more likely. The tensile force shows large-scale fluctuations. The cooling effect is more pronounced in this case and may amount to 20% of the initial kinetic energy.

Experiments have shown that MD provides insight into many basic features of strain and failure without invoking major *a priori* hypotheses. The method directly confirms the existence of phenomena such as the generation and motion of dislocations, cooling caused by extension of the system, etc. On the other hand, it is necessary to emphasize once more that the processes involving a large number of atoms and/or requiring considerable times (as compared to the period of thermal vibrations of atoms) cannot be observed in MD experiments.

4. Investigation of the Rehbinder effect

In order to study the mechanism of adsorption-induced strength reduction (the effect of environment on mechanical behaviour due to the decrease in the free surface energy of the solid [26–28, 32–36]), atoms of a second component (A) were placed into the cavity of the crystal. In the initial state they covered the walls of the cavity (the internal surface of the crystal, Fig. 4). The physico-chemical conditions in the experiments were chosen to promote the Rehbinder effect.*

Firstly, both components were of similar nature (Lennard–Jones monoatomic molecules); secondly, the A–A interaction was substantially weaker than the B–B interaction ($\epsilon_{BB}/\epsilon_{AA} = 2$–$6$), i.e. environment A was more fusible and had a lower surface tension than the basic component. The energy of mixing $u_0 = (\epsilon_{AA} + \epsilon_{BB})/2 - \epsilon_{AB}$ varied from 0 to $2kT$. Finally the experiments were carried out at temperatures at which the B lattice was stable while the environmental atoms were mobile and, in particular, could desorb from

*The number of atoms in our systems was small and the observation time relatively short. Thus the absence of environmental effects in MD experiments does not necessarily mean the same for macroscopic systems; our goal was to provide sufficient conditions for the Rehbinder effect rather than to determine the necessary conditions.

the cavity walls ($kT \approx 0.2\epsilon_{BB} = (0.4 \text{ to } 1.2)\epsilon_{AA}$). In view of the short physical time of the experiments (about 10^{-11} to 10^{-10} sec), the migration mobility of A atoms was usually enhanced by attributing a smaller radius and lower mass ($m_A = m_B/2, r_0^{AA} = r_0^{BB}/3, r_0^{AB} = 2r_0^{BB}/3$) to them.

Macroscopially, under these conditions the Rehbinder effect may result both from contact with the liquid phase A and from adsorption of A atoms at the crystal/gas interface [37]. In the absence of the environmental atoms at the same temperature and strain rate the crystal showed only plastic flow in all the experiments.

The plastic flow in the presence of environmental atoms, as in their absence, was preceded by elastic deformation, generation and accumulation of defects and stress relaxation. No environmental effects were observed in the elastic region; they took place at the stages of defect accumulation and lattice rearrangement. Environment-induced strength reduction requires the presence of structural defects [38, 39] and does not occur in the case of perfect crystals (whiskers [40]). Therefore, not unexpectedly, the strength reduction in the experiments under consideration was not great (10 to 15%). The quantitative estimations of the energy aspects of failure will be given below.

This series of experiments was undertaken primarily to reveal the environment-induced qualitative changes in the atomic picture of strain and failure. It appeared that adsorption-active atoms often caused brittle cracking, i.e. the Rehbinder effect may be directly observed in computer studies. The strain behaviour in each particular experiment could hardly be exactly predicted, since it was dependent not only on the physicochemical variables having macroscopic analogues (temperature, strain rate, number and mass of atoms and the interaction potential parameters) but also on essentially microscopic initial data such as the initial atomic velocities, the overall kinetic energy and the function of distribution of velocities being the same. The above variability of results is even more pronounced here. At the same time one may still single out a few principal mechanisms which sometimes operate in their pure form, though more often deformation shows features of several mechanisms.

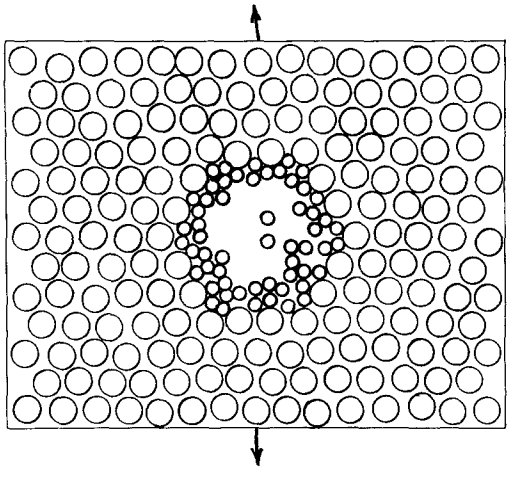

Figure 4 The initial positions of the atoms in the experiments on the Rehbinder effect.

(1) If the environment atoms possess high migration mobility, they penetrate into the strained and thus loosened lattice of the B component so that a crack filled by A atoms is formed (Fig. 5, upper part). The crack propagates as the foreign atoms penetrate to its tip. This migration is sharply accelerated by mechanical stress. At zero stress no diffusion of A particles was observed in this series of experiments. An estimation in terms of activation energy shows (see Section 6) that deformation may bring about a 200-fold increase in the diffusion rate of A atoms.

(2) By interacting with the environment, the B atoms become more mobile, and a two-component mixture forms in the stress concentration area. The mixture, which has no lattice and consists of very mobile atoms, may evidently be regarded as a liquid resulting from local melting or from dissolution of the basic component in the liquid environment. On stress relaxation, the B atoms either add to the lattice or remain in the solution. During stress relaxation A atoms were sometimes expelled from the lattice into the cavity, since their solubility substantially increased with strain (see Section 6).

(3) The environmental atoms of limited migration mobility (for instance, large atoms $r_0^{AA} = r_0^{AB} = r_0^{BB}$) could display their effect without mutual dissolution of the components. In this case an empty crack forms (Fig. 6, upper part), while the A atoms responsible for its generation stay in the crack mouth or "spread" into the adjacent area. Though the crack tip contains no A atoms, their presence in the system does promote crack propagation and makes it more likely than plastic flow. Significantly, in our model the interaction of each pair of atoms is

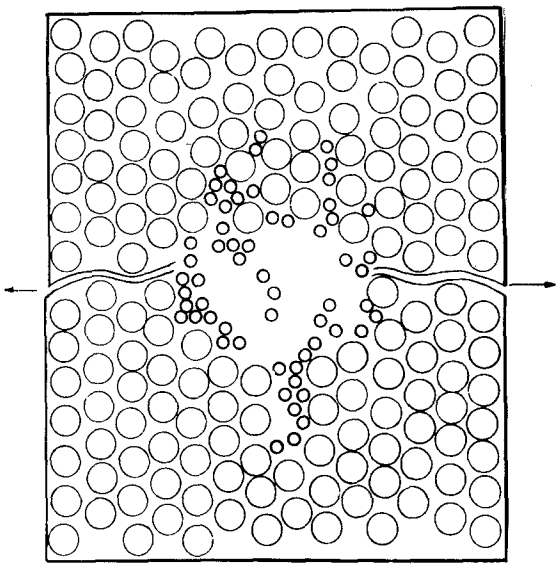

Figure 5 Penetration of A atoms into the lattice and formation of a crack filled by foreign atoms.

a function of distance only and does not depend on the presence and nature of neighbours. Hence the weakening of bonds between the basis component atoms cannot account for the observed effect of the environment. Rather, the generation and propagation of a crack is facilitated by the force acting on the activity walls normal to the crack and created by the A atoms. This force may on the average amount to 70% of the A–B bond strength and sometimes even exceed it. It may apparently be regarded as a form of two-dimensional pressure equal to the environment-induced decrease in the free surface energy of the solid. Special studies on this phenomena are described in Section 5.

(4) When the strain rate is high $[0.3(\epsilon_{BB}/m_B)^{1/2}]$ it takes about $3r_0^{BB}(m_B/\epsilon_{BB})^{1/2}$ time units (5 to 10 atomic thermal vibration periods) for the tensile stress to reach the strength of the sample. Even such small environment atoms as $r_0^{AA} = r_0^{BB}/3$ show no appreciable penetration into the lattice. Moreover, since the thermal motion of A atoms does not catch up with strain, they may act as a strengthening solid film. By strengthening the surface layer and preventing generation of dislocations the environment, in some cases, leads to the formation of an isolated crack in the bulk of the neck.

(5) Along with striking environment-induced embrittlement, more sophisticated strain behaviour was observed, as well as the absence of any effect of the second component (compare the upper and lower parts of Fig. 6).

It is therefore clear that a variety of molecular mechanisms are involved in environmental effects and that the macroscopic physico-chemical conditions affect the *probability* of a particular unit act of strain and failure in the presence of the environment. The behaviour of a real macroscopic sample is averaged over many such unit acts. For instance, if both plastic flow and brittle failure could occur at the crack tip with commensurate probabilities, macroscopically one should expect crack propagation involving certain plastic flow.

Fig. 7 shows the strain dependences of the overall energy of B–B and A–B atomic inter-

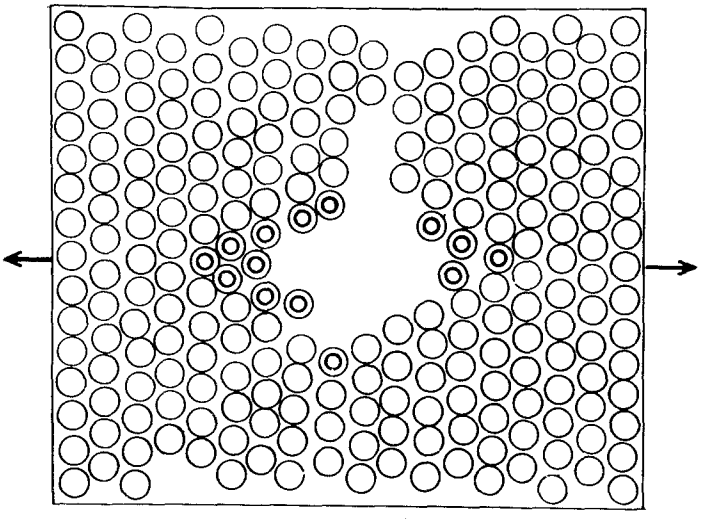

Figure 6 Formation of an empty crack (above) and plastic shear (below).

action, the work of the applied force* and temperature in an experiment with 60 A atoms and the following values of the parameters: $\epsilon_{AA} = \epsilon_{BB}/6$, $\epsilon_{AB} = \epsilon_{BB}/2$, $r_0^{AA} = r_0^{BB}/3$, $m_A = m_B/2$, the box elongation rate $0.03(\epsilon_{BB}/m_B)^{1/2}$, which are typical of mechanisms I and II, which in terms of energy are almost identical.

The overall variation of interaction energy B–B ($\Delta V_{BB} = 10\epsilon_{BB}$) and A–B ($\Delta V_{AB} = -5\epsilon_{BB} = -10\epsilon_{AB}$) may be compared with the work required for the creating of a new surface in a single-component system and with the adsorption-induced decrease in free energy of this surface. In other words, while 10 B–B bonds were broken in this experiment, 10 A–B bonds formed.

During deformation the number of A–B bonds increases as the environment penetrates the lattice or dissolves the solid. This process is simultaneous to that of B–B bonds breaking and rearranging and they mutually facilitate one another. Note that the number of A–B bonds is the greatest (the minimum of Curve 2) precisely at the moment when the system overcomes the potential barrier (the maximum of the B–B interaction energy curve). Only a part of the energy necessary to overcome this barrier comes from the applied force, while the rest results from the formation of new A–B bonds and from cooling of the system also observed in this case. Stress relaxation involves partial desorption of A atoms and their expelling from the lattice, as well as the addition of B atoms to the lattice. Due to these processes the number of A–B bonds somewhat decreases. From the energy standpoint the effect of environment may generally be described as follows: foreign atoms promote the rearrangement of the basic component atomic bonds which otherwise would have been impossible due to lack of energy. In other words, the environment decreases both the work necessary for failure and the potential barrier of failure.

Our MD experiments have thus shown that rapid (taking $\lesssim 10^{-10}$ sec) local processes involving just a few tens or hundred atoms may cause a transition from plastic flow to brittleness. MD has made it possible to observe the live picture of strain and failure in the presence of foreign atoms and to demonstrate its local variability, i.e. the

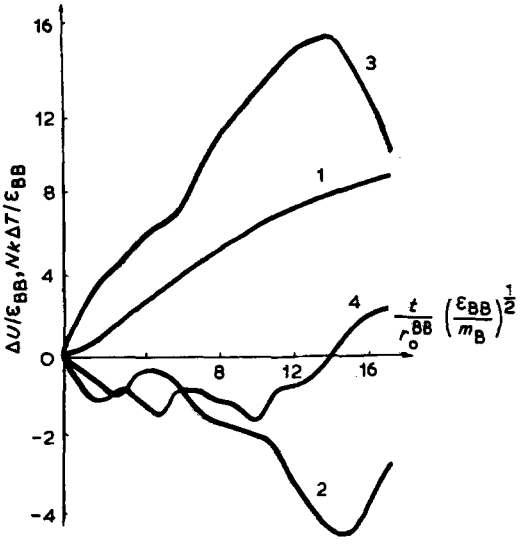

Figure 7 Deformation-induced variations in the overall energy of the system i.e. the work of the applied force (1), in the overall energy of interaction between the basic component atoms and the foreign atoms (2), in the B–B overall interaction energy (3), and in the kinetic energy of the system (4).

fact that under identical physico-chemical conditions a variety of environmental effects is possible. The microscopic analysis of the Rehbinder effect should therefore take into account that brittle failure of a macroscopic sample may result from a number of mechanisms operating at the crack tip. The following two conditions are common to all the mechanisms: (1) the solid–environment interaction must be strong enough, which macroscopically corresponds to the decrease in the surface free energy of the solid in contact with the environment [41, 42], and (2) thermal fluctuation must directly participate in the rearrangement of atoms at the crack tip in the presence of foreign atoms which, in turn, must possess sufficient mobility. This means that environment-induced brittle failure, in contrast to regular brittleness, is essentially a thermally activated process.

The analysis of our results should allow for the following circumstances. First, our calculations were based on paired potentials, i.e. the interaction between each pair of atoms did not depend on the presence and type of their neighbours. Second, MD calculations deal with only a few hun-

*The overall energy of the system minus the work of the applied force is constant during the experiments. The variation of the sum of the kinetic and the potential energy is equal to the work of the forces applied to the mobile walls of the box.

dreds of atoms and with times of about 10^{-10} sec. The above-discussed results indicate that even under such conditions one can observe the ductile-to-brittle transition and strength reduction. However, the Rehbinder effect may of course also involve some molecular mechanisms different from those observed. In particular, the atomic bonds of the solid may be directly weakened in the presence of environmental particles. An important role may be also played by slow and/or large-scale processes. The former factor appears to be a suitable object of MD studies allowing for the non-additivity of interaction. The latter factor is to be investigated by means of more macroscopic methods, where the MD approach may prove useful for the evaluation of microscopic parameters in macroscopic models.

5. Interaction of environment with crack walls

It has been shown in Section 4 that embrittlement does not necessarily involve the penetration of environment atoms into the lattice. This type of strength reduction has been studied in a special series of experiments. The system investigated is shown in Fig. 8. The crack walls were simulated by two rows of immobile B atoms. The CD wall (Fig. 8) served as a reflector limiting the cavity. As shown by Grivtsov, such a wall may be regarded as a model of a gas phase of density equal to that of the gas near the reflecting wall inside the cavity [6]. The interaction potential parameters were preset as $\epsilon_{AA} = \epsilon_{AB} = \epsilon$; $r_0^{AA} = r_0^{AB} = r_0$ (since the B atoms were immobile, no B–B potential was preset). The number of mobile A atoms corresponded to half the density of a hexagonal crystal with the lattice parameter r_0. The force of interaction between the mobile and the immobile atoms, the kinetic energy, the potential energy and the local density distribution were measured.

At high temperatures ($kT/\epsilon = 1.23$ and 0.74), the A component behaves as a dense gas, since all its atoms are mobile and uniformly distributed over the cavity volume. Adsorption of A occurs via interaction with the four closest B atoms at the crack tip, but no condensation area may be singled out. As the temperature decreases to $kT/\epsilon = 0.55$, the A atoms still possessing migration mobility gather near the crack tip which process may be regarded as condensation into a liquid. At $kT/\epsilon = 0.52$, three A particles are virtually fixed at

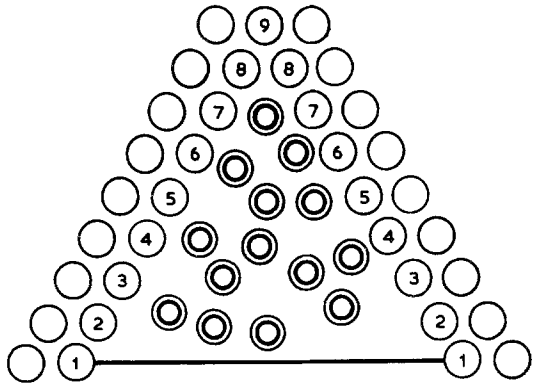

Figure 8 The system for the investigation of interaction between the environment atoms and the crack walls.

the lattice sites depending on the geometry of the walls while atoms further away show a marked tendency to a regular lattice arrangement, though still retain some mobility. In other words, in the kT/ϵ range from 0.55 to 0.52, crystallization occurs, as is evidenced also by the sharp increase in the heat capacity of the system in this temperature range.

Our calculations have shown that by interacting with the B atoms at the crack tip the environmental atoms create a force (on the average, $\bar{\lambda}_i$ per one B atom) which in effect "spreads" the walls of the crack and promotes its propagation. This force seems to be analogous to the two-dimensional pressure (one-dimensional in our case) of environment atoms on a solid surface, which is equal to the decrease in the surface free energy of the solid in contact with the environment. Table I gives average values of the force projected normal to the crack direction. This

TABLE I Average values of the forces acting upon the atoms of the solid from the environmental atoms in the direction normal to the crack axis (minus the pressure force of the gas measured from the pulse acting on the reflecting wall). The force values are given in interatomic bond strength units and are averaged over the corresponding atoms at the opposite sides of the crack. The numeration of atoms is the same as in Fig. 8. The last column gives the overall force promoting the crack propagation.

kT/ϵ	Numbers of atoms						
	3	4	5	6	7	8	Σ
1.23	0.0	−0.1	0.0	0.4	0.5	−0.2	0.6
0.74	0.0	−0.1	0.0	0.4	0.6	0.0	0.9
0.55	0.0	0.1	0.2	0.4	0.7	0.2	1.6
0.52	0.0	0.1	0.4	0.4	0.5	0.1	1.5

force may exceed half the strength of the A–B bond and, provided the A–B interaction is not substantially weaker than the B–B interaction, it may decrease the strength of the solid. Moreover, the values of λ_i are subject to pronounced fluctuation and at certain moments may exceed the A–B bond strength. Thus the environmental atoms may affect strain and failure even without outrunning the crack.

It is of interest to consider $\bar{\lambda}_i$ as a function of temperature. As the system cools down from $kT/\epsilon = 1.23$ to $kT/\epsilon = 0.55$ the maximum value of $\bar{\lambda}_i$ grows steadily, which means the condensation of the dense gas into a liquid at the crack tip enhances the effect of the environment. Further cooling to $kT/\epsilon = 0.52$ and the subsequent crystallization of the environment at the crack tip causes a sharp decrease in the force and, hence, weakens the effect. This trend provides further support for our earlier conclusion [37] that for the Rehbinder effect to occur the crack tip must contain a dense system of particles possessing sufficient mobility, i.e. a liquid phase or an adsorption layer. Both the decrease in concentration of the foreign atoms (at high temperatures) and the decrease in their mobility (at low temperatures when these atoms are arrested at lattice points) cause the decrease in the force acting on the crack walls.

6. Influence of elastic strain on mobility and heat of dissolution of interstitial admixtures

The effect of environmental penetration into the prefailure zone and the acceleration of this process in tension were mentioned in Section 4. The influence of tensile stress on the mobility of a second component in a crystal has been studied in a special series of calculations concerning diffusion of an interstitial admixture in an ideal lattice strained in an elastic manner.

The use of the MD approach in solving this problem would have required very long count times and would have given no opportunity to study a wide range of parameters of the system.* We have therefore employed the method of relaxation [43] which makes it possible to calculate the atomic structure equilibrium at 0K, the energy of this structure and the height of the potential barrier to be overcome by a foreign atom moving from one interstitial position to another. This height is identified as the activation energy of thermofluctuational diffusion transfer [44]. According to the Gibbson–Vineyard approach, the equations of motion of the particles are integrated from a certain non-equilibrium position of the atoms to the moment when the kinetic energy of the system starts to decrease. At the moment when the kinetic energy of the system has a maximum value (and the potential energy has a minimum value) the velocities of all the atoms are put equal to zero (or a very small value) and integration continues. The procedure is repeated until the maximum kinetic energy decreases below a certain preset value ($10^{-4}\epsilon_{BB}$ in our case) characterizing the accuracy to which the minimum of potential energy is reached. The summit of the potential barrier was determined using the following algorithm. At every step, after the force applied to a moving atom was calculated, the sign of its projection on the direction of displacement was changed so that the atom was "drawn" to the summit of the barrier rather than "rolled down" from it. This approach makes it possible to find the position of the barrier and its height without the routine calculation of intermediate states of the atom as it is assumed fixed in a number of points along its displacement path. Control calculations by means of the usual method demonstrated that the barrier in the system under consideration is of a simple one-maximum shape and that the method described is valid for determining its height.

The system studied (Fig. 9) consisted of 59 B atoms and one A atom. Strain was accomplished as described above and varied from almost limiting

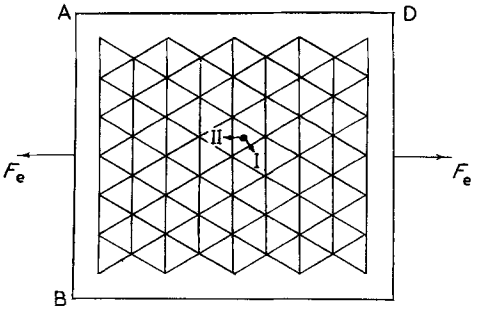

Figure 9 The positions of atoms in experiments on stress-induced variations in the mobility of interstitial admixtures. Arrows indicate Type 1 and Type 2 jumps.

*As mentioned in Section 4, during deformation the environmental atoms penetrate only into a strained lattice. A study of diffusion under zero stress would have required far longer count times.

extension to the same absolute value of compression. The A–B interaction potential parameters varied over the following range: r_0^{AB}/r_0^{BB} from 0.53 to 0.63 and $\epsilon_{AB}/\epsilon_{BB}$ from 0.5 to 1.5. Fig. 10 shows the activation energy of diffusion against parameters of the potential in the absence of strain.

Due to uniaxial strain, the symmetry of the crystal is distorted and the directions of displacement of interstitials become non-equivalent. In this system a distinction is made between the jumps at 60° to the strain axis (Type 1) and along the axis (Type 2). As is shown in Fig. 9, consecutive jumps of Type 1 result in diffusion oriented normally to the strain axis. Type 2 jumps may take the atom no farther than to a neighbouring triangular cell. The diffusion along the strain axis occurs via alternating jumps of Type 1 and Type 2.

Tensile stress facilitates Type 1 jumps and hinders Type 2 jumps; the effect of compression is to reverse this. Fig. 11 presents the dependence of the corresponding activation energies on applied stress for $r_0^{AB}/r_0^{BB} = 0.63$. While the mobility of large foreign atoms is very stress-sensitive, at $r_0^{AB}/r_0^{BB} = 0.53$ the activation energy of diffusion is almost independent of stress, particularly for Type 2 jumps. The values of the activation area $s_a = -(\partial E/\partial p)|_{p=0}$ where E is activation energy, p is stress (in $\epsilon/(r_0^{BB})^2$ units) are given in Table II.

The effect of stress compatible to the strength of the crystal may be quite striking. Thus, under the conditions of the studies of the Rehbinder effect described in Section 4, the acceleration of diffusion $D(p)/D(p=0) = \exp(\Delta E/kT)$ must be

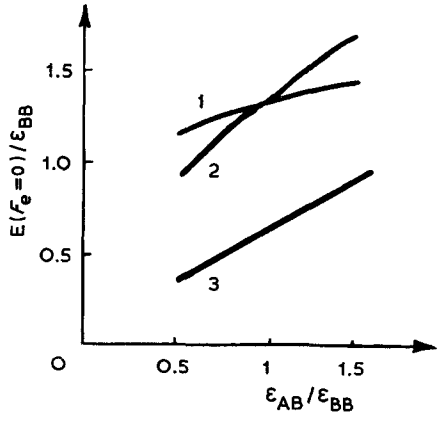

Figure 10 The activation energy of diffusion plotted against the A–B interaction potential parameters. $r_0^{AB}/r_0^{BB} = 0.63$ (Curve 1), 0.58 (Curve 2) and 0.53 (Curve 3).

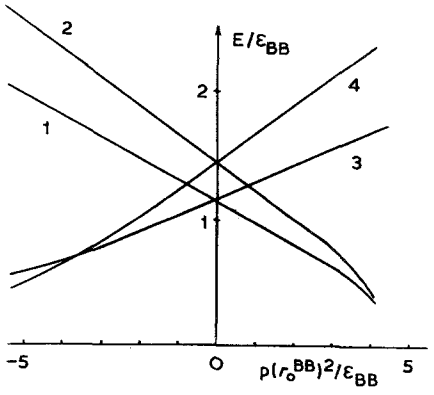

Figure 11 Dependence on activation energy of Type 1 (Curves 1 and 2) and Type 2 (Curves 3 and 4) diffusion jumps of an interstitial admixture plotted against uniaxial stress; $r_0^{AB} = 0.63 r_0^{BB}$; $\epsilon_{AB}/\epsilon_{BB} = 0.5$ (Curves 1 and 3) and 1.5 (Curves 2 and 4).

no less than two orders of magnitude. This is why the migration of foreign atoms in the MD calculations occurred only in the tensile stress concentration areas. In real systems, particularly in metals, the E/kT value is high and the effects may be even more dramatic, i.e. at stresses close to ideal strength the diffusion rate may increase by 3 to 4 orders of magnitude.

It should be noted that tensile stress promotes migration in the direction normal to the strain axis, which is most prone to cracking. (At the same time the diffusion along the strain axis, due to which the adsorption-active atoms flow away from the crack tip, decelerates).

The mobility of A atoms forming a substitutional solution appears to be strain-sensitive in the same manner. It was at least shown that uniaxial deformation offers strong influence on the mobility of vacancies in α-iron [45]. An interesting fact observed in [45] is that hydrostatic deformation produces a relatively minor effect because of mutual compensation of the influences of deformations along different axes.

Our results indicate that a similar situation must be observed for interstitial admixtures.

Our calculations have also given an estimation of the heat of dissolution of A atoms in the crystal. The heats of dissolution plotted against strain are shown in Fig. 12. If the foreign atom is larger than the interstitial cavity $[r_0^{AB}/r_0^{BB} > (3)^{1/2}/3]$ and thus creates a compression area around it, the tensile stress increases the heat of dissolution (the heat resulting from dissolution is assumed positive) and the compressive stress

TABLE II The activation area of diffusion of interstitial admixture atoms for type 1 (upper line) and type 2 (lower line) jumps.

r_0^{AB}/r_0^{BB}	$\epsilon_{AB}/\epsilon_{BB}$				
	0.50	0.75	1.00	1.25	1.50
0.53	0.05	0.06	0.07	0.08	0.09
	− 0.006	− 0.007	− 0.008	− 0.009	− 0.01
0.58	0.11	0.125	0.135	0.145	0.15
	− 0.055	− 0.065	− 0.075	− 0.085	− 0.095
0.63	0.16	0.18	0.19	0.20	0.21
	− 0.125	− 0.15	− 0.175	− 0.195	− 0.215

decreases this heat. The effect for small A atoms ($r_0^{AB}/r_0^{BB} < (3)^{1/2}/3$) is reversed and weaker. If the solubility of A in the solid phase is poor and one can assume that $\Delta c/c_0 = \exp(\Delta H/kT) - 1$ (c_0 is the solubility in the absence of stress and Δc is the change in solubility under the effect of stress), the observed variation in the heat of dissolution may cause drastic changes in solubility, particularly for large interstitial atoms in a stretched lattice. The Rehbinder effect may be very sensitive to this factor. If, prior to deformation, the liquid and the solid phases were mutually saturated, the applied tensile stress which changes the solubility of the environment and increases the mobility of its atoms promotes the flow of foreign atoms to the crack tip. This, in turn, decreases still more the surface free energy of the solid–liquid interface [46].

7. Long-term strength of a unit interatomic bond

Static fatigue behaviour, when the load applied to the sample does not suffice for instant failure, is particularly dependent on thermal fluctuations.

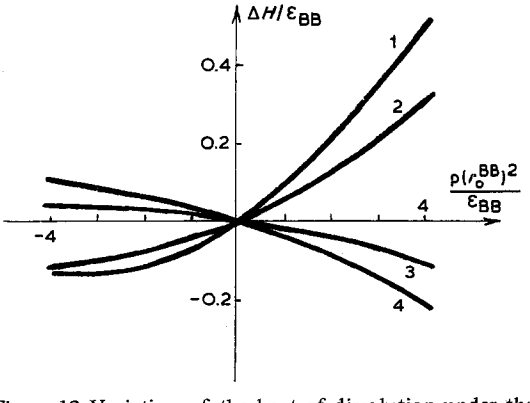

Figure 12 Variation of the heat of dissolution under the effect of uniaxial stress for an interstitial admixture with $\epsilon_{AB}/\epsilon_{BB} = 1.5$ (Curves 1 and 4) and 0.5 (Curves 2 and 3); r_0^{AB}/r_0^{BB} equals 0.63 (Curves 1 and 2) and equals 0.53 (Curves 3 and 4), respectively.

Many years of research, notably by Zhurkov and his school, have shown (see for instance, [47–58]) that the long-term strength (durability, τ_m) of a material under a constant load is described by a universal correlation

$$\tau_m = \tau_0 \exp[(U_0 - \gamma p)/kT], \qquad (1)$$

where τ_0, U_0 and γ are parameters. This equation is applicable to many materials under a broad range of experimental conditions. Several workers, in particular Bartenev *et al.* [53, 54], have shown that this correlation may be inferred from the idea that the interatomic bond failure and the unit act of crack propagation involve a thermofluctuational mechanism, assuming that the activation energy of failure is a linear function of local stress or of the force applied to the bond being broken. They have also established a relationship between the values in Equation 1 and the microscopic parameters of the material. Independent determination of the parameters of Equation 1 and the verification of the above assumptions on thermofluctuational mechanism of failure and the linear relationship between the activation energy and the applied stress require atomic-scale studies of unit acts of failure.

This part of the paper concerns the investigation of the long-term strength of a unit interatomic bond in a two-dimensional system [21]. (A similar study for a one-dimensional chain was carried out somewhat later by Zaitsev and Razumovskaya [59]). We have considered the system consisting of two contacting crystals (Fig. 13). The average kinetic energy of the atoms (kT) was equal to 0.09 (see Section 2; for argon this corresponds to 10.8 K). In contrast to the above-described experiments (Sections 3 and 4) where the mobile walls were moving at a constant velocity, in this series they moved as particles of mass $7m$ under the effect of interaction with the atoms of the crystal and the applied force F_e. A series of 64 experi-

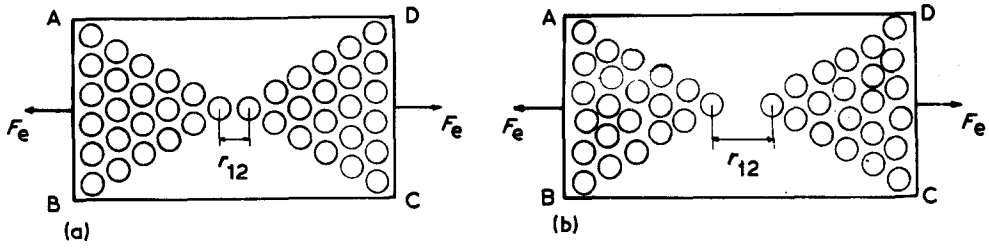

Figure 13 Positions of atoms (a) before and (b) after bond failure.

ments with different sets of random initial velocities of atoms was performed for each value of F_e; the mean square deviation of the average time to failure was not greater than ± 13%.

No failure was observed for a certain time after the beginning of the experiment. The potential energy and the kinetic energy were fluctuating about their average values. The average force of interaction between the atoms and the mobile walls was equal to the applied force, and the walls were vibrating about the equilibrium position corresponding to the preset value of F_e and kT. The work of the applied force was on average close to zero.

At a certain moment failure occurred, primarily by rupture of one crystal from the other (Fig. 13b). The force of interaction between the molecules and the mobile walls decreased and the walls together with the crystals started to move apart irreversibly under the effect of the applied force. The temperature of the system increased, though only slightly ($\sim 0.01\,\epsilon$). The work of the applied force spent on the failure was close to ϵ. It was assumed that failure occurred when the value of r_{12} (Fig. 13) reached $1.57\,r_0$, as the broken bond was never restored in our experiments after this criterion had been fulfilled.

The calculations confirmed that the failure of a unit bond in the system under consideration is fluctuational and obeys universal statistical laws. To within the experimental error the probability that a bond does not fail during time t proved equal to $\exp(-t/\bar{\tau})$, where $\bar{\tau}$ is the average time to failure under the given conditions. The system deviated from this behaviour only under high loads ($F_e \geqslant 0.8\,F_m$), when the failure occurred rapidly enough [$\bar{\tau} < 10\,r_0(m/\epsilon)^{1/2}$] and the equilibration time as well as the time necessary for the crystals to move apart until the criterion of failure is fulfilled became compatible with the fluctuation expectation time.

These experiments revealed that the long-term strength in the system under consideration obeys Zhurkov's equation ($\ln\tau$ is a linear function of the applied force, Fig. 14a), and the parameter γ, as one would expect in the absence of defects and stress concentration, is compatible with the interatomic distance and equals $r/3$.*

In Fig. 14b durability is compared with the energy (ΔU) required to break a bond stretched by a force F_e (see Fig. 15). The results obey a correlation $\ln\tau = \ln\tau_0 + \Delta U/kT$, which confirms the thermal fluctuation mechanism of failure and makes it possible to estimate τ_0 as $0.13\,r_0(m/\epsilon)^{1/2}$

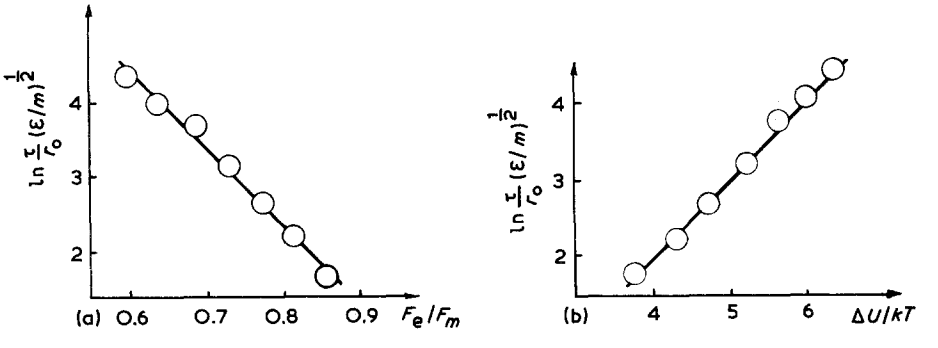

Figure 14 Durability of a bond plotted against (a) the applied force and (b) the energy necessary for the failure.

*Since a unit bond fails in our model, we operate with force rather than with stress. Accordingly, the parameter γ has the dimension of length rather than volume (in a three-dimensional system) or area (in a two-dimensional system).

(3.2×10^{-13} sec for argon). Being close in order of magnitude to common values of τ_0 in Equation 1, this value is equal to one fifth of the average vibration period of the r_{12} bond.*

Incidentally, the bond failure requires that the increase in r_{12} be correlated with the motion of neighbouring atoms. In a number of experiments the bond length became greater than the "critical" value r'' (Fig. 15) and the attraction force between the crystals became lower than F_e, but the bond did not fail during the given vibration because in a few hundredths $r_0(m/\epsilon)^{1/2}$ the distance r_{12} decreased again due to the thermal motion of the atoms.

Over the range of F_e values studied the dependence of ΔU on F_e is virtually linear (Fig. 15), which means that the principal assumption of static fatigue theories is fulfilled and $d(\Delta U)/dF_e \approx -r_0/3$. Hence the validity of Equation 1 and the value of γ calculated.

Our experiments have thus demonstrated that a unit act of failure (the failure of an interatomic bond) obeys a thermal fluctuation mechanism and the long-term strength depends on the correlation between the energy necessary to break a bond in tension and the energy of thermal vibrations of the atoms. Specifically, the fact that the attraction of the crystals becomes lower than the applied force does not suffice for the bond to fail. Another important feature is that the characteristic period, τ_0, is essentially shorter than the period of the bond length vibration. These results may be useful in developing a microscopic physico-chemical theory of the strength of disperse structures, where thermal fluctuations are crucial to the failure of contacts between individual particles.

8. Formation and failure of unit phase contacts between crystals

Along with the failure of contacts between disperse phase particles, the formation of such contacts, e.g. in sintering, is also a topical problem of physico-chemical mechanics. The development of phase contacts has been described theoretically (see review [60] and a more recent paper on computer simulation using continual approximation [61]). However, the initial stages of the agglutination of crystals (the transformation of a point contact into a phase contact) are not easy to investigate. The point contact contains a surface singularity and the discrete atomic structure in this area has to be taken into account. On the other hand, the small number of atoms in the contact zone suggests that MD may prove very appropriate for the investigation of the initial stages of sintering. The authors undertook such an investigation in co-operation with Sokolov.

The system studied contained two crystals with a point contact between them (Fig. 16a). The immobile walls used in the above-described experiments were replaced by periodical boundary conditions, which meant the system was assumed to border on the same cells from the top and from the bottom. In such a mode, which is widely used in MD studies, there are no laterial faces to

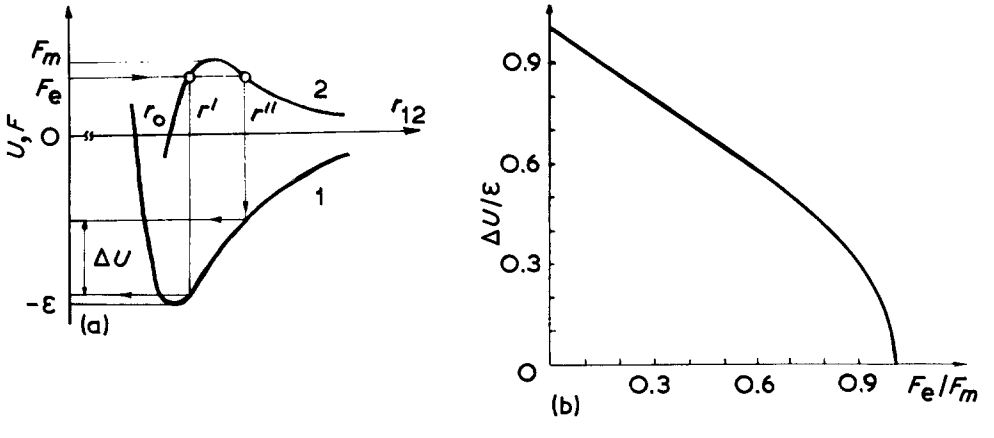

Figure 15 (a) the dependence of the energy (1) and the force (2) of interaction between the crystals on r_{12}, (b) ΔU as a function of F_e.

*The average vibration period of a bond length was calculated using an autocorrelation function $\varphi(t) = \langle (r_{12}(t) - \bar{r}_{12}) \times (r_{12}(O) - \bar{r}_{12}) \rangle$. The distance between the maxima of this function corresponds to the average vibration period, which under the given conditions was equal to $0.66\, r_0(m/\epsilon)^{1/2}$.

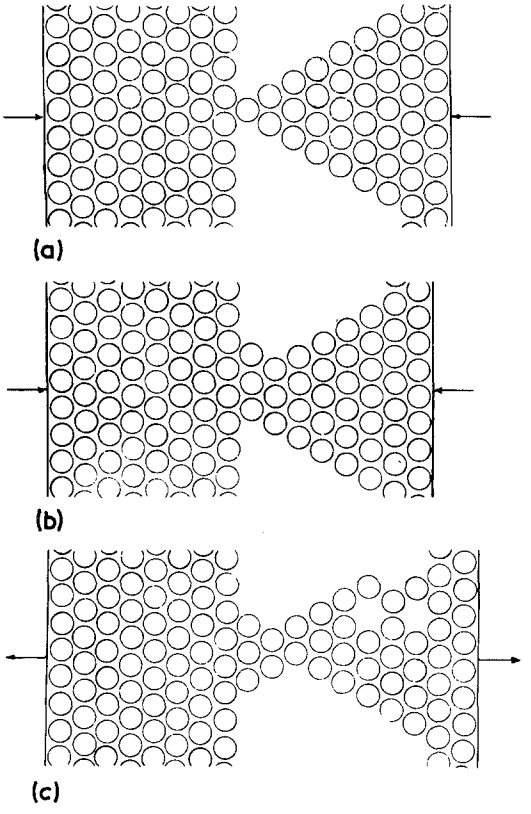

Figure 16 Positions of atoms (a) in the beginning of the experiment, (b) after formation of a unit phase contact, (c) plastic flow during the failure of a unit phase contact between the crystals.

affect the behaviour of the microcrystal. "Sintering" was performed under a constant compressive load below the melting point of the two-dimensional crystal ($kT_m \approx 0.4\epsilon$). The expectation time of a unit phase contact formation (Fig. 16b) and the mechanisms of sintering were determined at various values of F_e and kT.

Within a certain range of experimental conditions ($|F_e| < 5\epsilon/r_0$ and $kT/\epsilon < 0.3$) sintering proved to obey a thermal fluctuation mechanism in the same manner as the failure of a unit bond did in Section 7. Fig. 17 gives the dependence of the average time of expectation of a unit act of sintering on the force of compression and on temperature. At $kT/\epsilon < 0.3$ and $|F_e|r_0/\epsilon < 6$, the results may, to within the experimental error, be described* by Equation 1, with the following values of its parameters: $U_0 = 0.8\,\epsilon$; $\gamma = 0.12\,r_0$; $\tau_0 = 1.5\,r_0(m/\epsilon)^{1/2}$. In this process τ_0 is greater by an order of magnitude than the characteristic time of failure of an interatomic bond $(0.13r_0(m/\epsilon)^{1/2}$, see Section 7) and is equal to 3 to 4 periods of vibration of the lattice atoms.

These experiments also demonstrated the variability of the microscopic behaviour. The values of kT and F_e being identical, the unit phase contact appeared on account of different arrangements of atoms. Within the area under consideration two mechanisms were of major importance, namely (1) the penetration of an atom forming the wedge vertex between two atoms of the second layer and (2) the movement of this atom along the surface of the second crystal, while the crystals were brought closer together under the effect of attraction and the applied force.

The total expectation time is equal to $\bar{\tau} = 1/(\Sigma\bar{\tau}_i^{-1})$, where $\bar{\tau}_i$ is the average expectation time of a unit act according to the ith mechanism. Thus, the operation of two or more competing mechanisms may result in deviation from Equation 1. In our experiments Mechanism 1 was observed far more frequently than Mechanism 2 ($\bar{\tau}_1 \ll \bar{\tau}_2$), and the experiments did not permit any definite conclusions about deviations from Equation 1 and on the correlation between $\bar{\tau}_1$ and $\bar{\tau}_2$.

At compression forces above a certain value ($6\epsilon/r_0$ at $kT/\epsilon = 0.17$) the microscopic behaviour changed, so that sintering took place via deformation of the crystals. This, however, resulted in the same unit phase contact as that shown in Fig. 16b. (The wedge vertex atom penetrated into

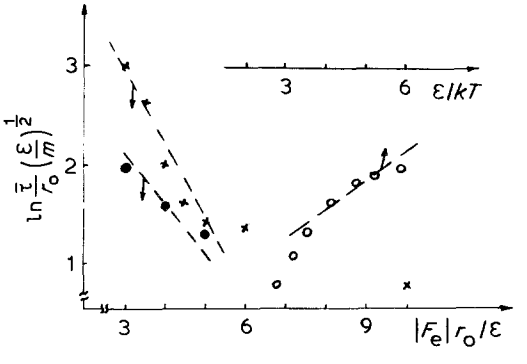

Figure 17 The dependence of $\ln[\bar{\tau}/\tau_0(\epsilon/m)^{1/2}$ on the compression force at $kT/\epsilon = 0.17$ (x) and 0.25 (•) and on temperature at $|F_e|r_0/\epsilon = 4$ (○). Dotted straight lines correspond to an equation $\ln[\bar{\tau}/\tau_0(\epsilon/m)^{1/2} = 0.4 - (0.8\,\epsilon - 0.12|F_e|r_0)/kT$.

*An average of 15 experiments was carried out for each set of parameters. Thus the mean square deviation of $\bar{\tau}$ is about $\bar{\tau}/4$, and the error in determining $\ln\bar{\tau}$ about ± 0.25.

the second crystal and expelled one of its surface atoms into the contact zone). The value of $\bar{\tau}$ in this case is greater than predicted by Equation 1 simply because the atoms lack time for their rearrangement, considering also the criterion chosen for the end of the process: 3 atoms of the wedge were to enter the first co-ordination sphere of the second crystal atoms. As the temperature was raised to $kT/\epsilon > 0.3$ $(T/T_m > 0.75)$, the number of mechanisms of the elementary act of sintering grew sharply and the acceleration of the process was more pronounced than predicted from Equation 1. This is due to the beginning of local melting in the contact zone and to the high mobility of atoms (cf. the results [62] on the melting of surface layers of crystals at temperatures appreciably lower than T_m).

The failure of contacts was studied under constant extension rate conditions. The point contact failed under a stress of about $4\,\epsilon/r_0$. The wedge vertex atom in most cases remained attached to the plane, owing to its interaction with distant neighbours. Otherwise the lattices were not distorted. The unit phase contact failed under the stress of about 10 to $11\,\epsilon/r_0$ (75 to 80% of the stress necessary for simultaneous breaking of all the bonds in the thinnest cross-section). Along with brittle failure, when three atoms of the wedge were not separated from the flat crystal, plastic deformation of the wedge and neck formation were sometimes observed (Fig. 16c). This means microscopic phase contacts between plastic materials may fail in a plastic manner.

9. Conclusion

The use of the MD approach, which takes advantage of both theoretical and experimental methods, has made it possible to observe the actual behaviour of atoms in a crystal, their thermal motion, the unit acts of their rearrangement and interatomic bond failure, the effect of foreign atoms on mechanical behaviour and other phenomena. The approach, which does not involve any essentially simplifying models, proved valid for the investigation of such processes as elastic strain, plastic flow, formation of defects, local failure, and the adsorption and transfer of atoms. New quantitative estimations based on micromechanics of mechanical behaviour have been obtained. The MD approach has also suggested a number of qualitative conclusions, some of which are far from trivial. One of the most general results is the variability of the microscopic pictures observed and their essentially stochastic nature. Dealing with such small systems one observes unit acts of behaviour rather than the usual average phenomena.

The MD approach has also been used to study some other physico-chemical problems, such as the molecular picture of wetting and spreading. Computer experiments carried out for a variety of interactions between the support and the microscopic droplet resulted in all possible types of behaviour. On the background of surface fluctuations (Mandelshtam's waves) we observed the transition to complete wetting and spreading on a lyophilic surface (when the energy of adhesion was equal to that of cohesion): the formation of a segment with a finite contact angle on a lyophobic surface (90° when the energy of adhesion was equal to half that of cohesion) both by advancing and by receding. These experiments revealed the statistical nature of the contact angle and the dynamic equilibrium between the liquid phase and the adsorption layer on a solid surface. These experiments do not bear direct relevance to mechanical behaviour and they have not been included in this review; the reader may find the results in [14, 15].

The MD approach also provides an excellent opportunity of visualizing the molecular picture of the processes studied by means of cinematography. The data on the positions consequently occupied by atoms may be presented in a movie film with a 10^8 to 10^9 times "linear magnification" and 10^{11} times "time magnification" (deceleration). Such a film was first demonstrated by one of the authors at the plenary lecture during the 7th International Congress on Surfactants (Moscow, 1976).

At present the authors are continuing their studies on contact interactions (including those between disperse phase particles), particularly on the effect of the environment on the formation and failure of contacts, surface and near-surface defects. The approach is also being used to investigate three-dimensional systems and other types of interaction (ionic and metal interactions).

Acknowledgements

The authors wish to thank V. I. Spitsyn, S. N. Zhurkov, B. V. Deryaguin, A. N. Orlov, A. D. Sheluko, A. Westwood, R. Latanision, E. Wolfram, H. Sonntag, J. Padday, R. Oriani, R. Bullough and S. Brookes for their valuable comments on the

paper. These studies were performed thanks to the great opportunities in using computer time given to the authors by the Institute of Physical Chemistry of the USSR Academy of Sciences. The Russian original was translated into English by B. Kenzheev of Moscow University.

References

1. B. J. ALDER and T. E. WEINWRITE, *J. Chem. Phys.* **27** (1957) 1208; and in Proceedings of the International Symposium on Transport Processes in Statistical Mechanics, Brussels, August 1956, edited by J. Prigogine (Interscience, New York, 1958) p. 97.
2. A. RAHMAN, *Phys. Rev.* **A136** (1964) 405.
3. W. W. WOOD and J. J. ERPENBECK, "Annual Review of Physical Chemistry", Vol. 27 (Palo Alto, California, USA, 1976) p. 319.
4. A. M. YEVSEEV, M. I. SHAKHPARONOV and G. P. MISYURINA, *Zh. Fiz. Khim.* **44** (1970) 2999.
5. V. G. CHERVIN and A. M. YEVSEEV, *ibid.* **44** (1970) 2465.
6. A. M. YEVSEEV and M. YA. FRENKEL, "Sovremennye Problemy Fizicheskoy Khimii", Vol. 9 (MGU, Moscow, 1976) p. 3.
7. A. N. LAGAR'KOV and V. M. SERGEEV, *Teplofizika Vysokih Temperatur* **8** (1970) 1309.
8. *Idem, ibid.* **11** (1972) 513.
9. *Idem, ibid.* **13** (1975) 438.
10. A. G. GRIVTSOV, *Dokl. AN SSSR* **190** (1970) 868.
11. *Idem,* "Osnovnye Problemy Teorii Fizicheskoy Adsorbtsii' (Nauka, Moscow, 1970) pp. 347, 352.
12. A. G. GRIVTSOV and E. E. SHNOL', preprints of the Institute of Applied Mathematics, **3, 4** (1971).
13. D. V. FEDOSEEV, R. K. CHUZHKO and A. G. GRIVTSOV, "Geterogennaya Kristallizatsiay iz Gazovoy Fazy" (Nauka, Moscow, 1978).
14. V. S. YUSHCHENKO, A. G. GRIVTSOV and E. D. SHCHUKIN, *Kolloidn. Zh.* **39** (1978) 335.
15. E. D. SHCHUKIN and V. S. YUSHCHENKO, *ibid.* **39** (1978) 331.
16. V. S. YUSHCHENKO, A. G. GRIVTSOV and E. D. SHCHUKIN, *Dokl. AN SSSR* **215** (1974) 148.
17. V. S. YUSHCHENKO and A. G. GRIVTSOV, "Dinamika Dislokatsiy" (abstracts of papers of the IV All-Union Symposium) (FTINT, Kharkov, 1973) p. 6.
18. V. S. YUSCHENKO, A. G. GRIVTSOV and E. D. SHCHUKIN, *Dok. AN SSSR* **219** (1974) 162.
19. A. G. GRIVTSOV and V. S. YUSHCHENKO, *Fiz. Khim. Mekhanika Mater.* **12** (1976) 31.
20. V. S. YUSHCHENKO and E. D. SHCHUKIN, "Modelirovanie na EVM Defektov v Kristallakh", Vol. 1 (FTI, Leningrad, 1979) p. 168.
21. *Idem, ibid.* p. 166.
22. *Idem, Dokl. AN SSSR* **242** (1978) 653.
23. L. D. LANDAU and E. M. LIFSHITZ, "Statisticheskaya Fizika" (Nauka, Moscow, 1976) p. 1.
24. W. G. HOOVER, W. T. ASHURST and R. J. OLNESS, *J. Chem. Phys.* **60** (1973) 4043.
25. J. W. MARTIN and D. J. BACKON, *J. Nucl. Metall.* **20** (1976) 198.
26. P. A. REHBINDER and E. D. SHCHUKIN, *Usp. Fiz. Nauk* **108** (1972) 3.
27. E. D. SHCHUKIN, *Fiz. Khim. Mekhanika Mater.* **12** (1976) 3.
28. *Idem,* in "Surface Effects in Crystal Plasticity", edited by R. M. Latanision and J. F. Fourie (Noordhoff Publishing, Noordhoff–Leyden, the Netherlands, 1977) p. 701.
29. P.-O. ESBJORN and E. J. JENSEN, *J. Phys. Chem. Solids* **37** (1976) 1081.
30. E. J. JENSEN and P.-O. ESBJORN, *J. Nucl. Metall.* **20** (1976) 459.
31. D. N. BOLSHUTKIN, N. F. KULIK *et al.* "Trudy FTINT AN SSSR" Vol. 19 (FTINT, Kharkov, 1972) p. 9.
32. P. A. REHBINDER, V. I. LIKHTMAN and E. D. SHCHUKIN, "Fiziko-Khimicheskaya Mekhanika Metallov", (Nauka, Moscow, 1962).
33. YU. V. GORYUNOV, N. V. PERTSOV and B. D. SUMM, "Effekt Rebindera" (Nauka, Moscow, 1966).
34. W. ROSTOCKER, J. MCCOGIE and C. MARKUS, "Liquid Embrittlement", (Mir, Moscow, 1962) in Russian.
35. A. R. C. WESTWOOD, in "Surface Effects in Crystal Plasticity", edited by R. M. Watanision and J. F. Fourie (Noordhoff Publishing, Noordhoff–Leyden, 1977) p. 835.
36. *Idem,* in "Environment-Sensitive Mechanical Behaviour" edited by A. R. C. Westwood and N. S. Stoloff (Gordon and Breach, New York, 1966).
37. V. S. YUSHCHENKO, PhD. Thesis, Academy of Sciences of the USSR, Moscow, 1970.
38. E. D. SHCHUKIN, B. D. SUMM and YU. V. GORYUNOV, *Dokl. AN SSSR* **167** (1966) 693.
39. L. S. SOLDATCHENKOVA, YU. V. GORYUNOV, G. I. DEN'SHCHIKOVA, Z. M. POLUKAROVA, B. D. SUMM and E. D. SHCHUKIN, *ibid.* **203** (1972) 83.
40. V. N. ROZHANSKY, *Fiz. Tverdogo Tela* **2** (1960) 978.
41. E. D. SHCHUKIN and V. S. YUSHCHENKO, *Fiz. Khim. Mekhanika Mater.* **2** (1966) 133.
42. *Idem,* "Poverkhnostnye Yavleniya v Rasplavakh", (Naukova Dumka, Kiev, 1968) p. 415.
43. J. B. GIBSON, A. N. GOLAND, M. MILGRAM and G. H. VINEYARD, *Phys. Rev.* **120** (1960) 1229.
44. R. A. JOHNSON, *ibid.* **134A** (1964) 1329.
45. K. W. INGLE and A. G. CROCKER, *J. Nucl. Mater.* **69/70** (1978) 667.
46. A. A. ZHUKHOVITSKY, V. A. GRIGORYAN and E. MIKHAILIK, *Dokl. AN SSSR* **155** (1964) 2.
47. S. N. ZHURKOV and B. N. NARZULAEV, *Zh. Teor. Fiz.* **23** (1953) 1677.
48. S. N. ZHURKOV and T. P. SAPFIROVA, *Dokl. AN SSSR* **101** (1955) 237.
49. *Idem, Fiz. Tverdogo Tela* **2** (1960) 1034.
50. V. R. REGEL', *Zh. Teor. Fiz* **21** (1951) 287.
51. V. R. REGEL', A. I. SLUTSKER and E. E. TOMASHEVSKY, "Kineticheskaya Priroda Prochnosti Tverdykh Tel", (Nauka, Moscow, 1974).

52. G. M. BARTENEV, *Izv. AN SSSR, OTN* 9 (1955) 53.
53. G. M. BARTENEV and YU. S. ZUEV, "Prochnos' i Razrushenie Vysokoelastichnykh Materialov", (Khimiya, Moscow and Leningrad, 1964).
54. A. N. ORLOV, *Fiz. Tverdogo Tela* 3 (1961) 500.
55. B. YA. PINES, *Zh. Teor. Fiz.* 25 (1955) 1399.
56. *Idem, Fiz. Tverdogo Tela* 1 (1959) 265.
57. P. GIBBS and J. B. CULTER, *J. Amer. Ceram. Soc.* 34 (1951) 200.
58. D. A. STUART and O. L. ANDERSON *ibid.* 36 (1953) 416.
59. M. G. ZAITSEV and I. V. RAZUMOVSKAYA, *Vysokomolekulyarnye Soedinenia* 21B (1979) 461.
60. YA. E. GEGUZIN, "Fizika Spekaniya", (Nauka, Moscow, 1967).
61. P. BROSS and H. E. EXNER, *Acta Met.* 27 (1979) 1013.
62. J. Q. BROUGHTON and L. V. WOODCOCK, *J. Phys., C: Solid State Phys.* 11 (1978) 2743.

Received 15 May and accepted 10 June 1980.